Drug Design, Development and Therapy

Dovepress
open access to scientific and medical research

Open Access Full Text Article

ORIGINAL RESEARCH

High glucose inhibits ClC-2 chloride channels and attenuates cell migration of rat keratinocytes

This article was published in the following Dove Press journal:
Drug Design, Development and Therapy
28 August 2015
Number of times this article has been viewed

Fuqiang Pan
Rui Guo
Wenguang Cheng
Linlin Chai
Wenping Wang
Chuan Cao
Shirong Li

Department of Plastic and Reconstructive Surgery, Southwestern Hospital, Third Military Medical University, Chongqing, People's Republic of China

Background: Accumulating evidence has demonstrated that migration of keratinocytes is critical to wound epithelialization, and defects of this function result in chronic delayed-healing wounds in diabetes mellitus patients, and the migration has been proved to be associated with volume-activated chloride channels. The aim of the study is to investigate the effects of high glucose (HG, 25 mM) on ClC-2 chloride channels and cell migration of keratinocytes.

Methods: Newborn Sprague Dawley rats were used to isolate and culture the keratinocyte in this study. Immunofluorescence assay, real-time polymerase chain reaction, and Western blot assay were used to examine the expression of ClC-2 protein or mRNA. Scratch wound assay was used to measure the migratory ability of keratinocytes. Transwell cell migration assay was used to measure the invasion and migration of keratinocytes. Recombinant lentivirus vectors were established and transducted to keratinocytes. Whole-cell patch clamp was used to perform the electrophysiological studies.

Results: We found that the expression of ClC-2 was significantly inhibited when keratinocytes were exposed to a HG (25 mM) medium, accompanied by the decline of volume-activated Cl^- current ($I_{Cl,vol}$), migration potential, and phosphorylated PI3K as compared to control group. When knockdown of ClC-2 by RNAi or pretreatment with wortmannin, similar results were observed, including $I_{Cl,vol}$ and migration keratinocytes were inhibited.

Conclusion: Our study proved that HG inhibited ClC-2 chloride channels and attenuated cell migration of rat keratinocytes via inhibiting PI3K signaling.

Keywords: high glucose, keratinocytes, ClC-2, cell migration, PI3K

Introduction

Patients with diabetes mellitus (DM) often suffer from various metabolic abnormalities at tissue level, including many delayed wound healing situations that have been the leading cause of leg amputation.[1] Although a series of events leads to successful repair of acute wounds,[2] the underlying mechanism of these processes seem unavailable in chronic ulcers. The cause of chronic ulcers in DM patients has been attributed to a variety of abnormal biological mechanisms: ischemia, neuropathy, infection, increased proteases, prolonged inflammatory response, cytokine and growth factors deficits, etc.[3,4] It has been demonstrated that re-epithelialization is responsible for the delayed healing of wounds.[5] Both migration and proliferation of keratinocytes play essential roles in the re-epithelialization process to cover the cutaneous wound.[6,7] Accumulating evidence has demonstrated that migration of keratinocytes is critical to wound re-epithelialization and defects of this function result in delayed healing of wounds.[8,9]

Ion channels are expressed in a wide range of tissues and participate in different cellular functions, such as proliferation, volume control, enzyme activity, gene expression, secretion, invasion, and intercellular communication.[10] Volume-activated

Correspondence: Chuan Cao; Shirong Li
Department of Plastic and Reconstructive Surgery, Southwest Hospital, Third Military Medical University, 29 Gaotanyan Main Street, Shapingba District, Chongqing 400038, People's Republic of China
Tel/fax +86 23 6876 5551
Email ucccao@yeah.net; lishirong_cqzx@yeah.net

chloride channels (VACCs) are considered to respond as the activation of a volume-activated Cl^- current ($I_{Cl,vol}$) when they are stimulated by osmotic cell swelling. The outflow of Cl^- and K^+ through VACC and K^+ channels leads to a decrease in cell volume termed regulatory volume decrease (RVD).[11,12] Recently, alteration of VACC has been identified to play an important role in glioma cell metastasis.[13] Likewise, other studies have also demonstrated that VACC are involved in migratory capacity and cell proliferation.[14,15] A series of studies suggested that ClC-2 channels contributed to regulate cell volume and control intracellular Cl^- concentration.[16–18] However, whether ClC-2 channels contribute to cell volume regulation and then sequentially play a role in migratory defects of diabetes keratinocytes is still unknown.

We hypothesize that ClC-2 play an important role in the defects of keratinocyte migration and sequentially leading to delayed wound healing in DM patients. We found that the exposure of keratinocytes to a high glucose (HG, 25 mM) concentration significantly inhibited the ClC-2 expression, volume-activated Cl^- current ($I_{Cl,vol}$), migration potential, and phosphorylated PI3K as compared to the control group. Lentivirus-mediated RNAi knockdown of ClC-2 inhibits $I_{Cl,vol}$ and migratory abilities of keratinocytes. In order to identify the role of PI3K signaling in regulation of ClC-2, normal glucose (NG) keratinocytes were pretreated with 100 nM wortmannin. We found that it attenuates the CLC-2 expression, $I_{Cl,vol}$, and migration potential. These may lead to the development of therapies to promote healing of DM chronic ulcers.

Methods

Isolation and culture of keratinocyte

Newborn Sprague Dawley rats (Experimental Animal Center of Daping Hospital at the Third Military Medical University of Chongqing City, People's Republic of China) were used in this study in accordance with the ethical standards and animal protocols approved by the Institutional Animal Care and Use Committee at the Third Military University. Primary epidermal keratinocytes were isolated and cultured according to the modified methods described by Lan et al.[19] In brief, the skin of newborn rats from the back was obtained after sterilization and sequentially washed in phosphate-buffered saline (PBS); Thermo Fisher Scientific, Waltham, MA, USA) twice. The keratinocytes were harvested by centrifugation at 1,000 rpm for 10 minutes. The cell pellet was gently re-suspended in keratinocyte serum-free medium (K-SFM; Thermo Fisher Scientific), containing 25 ng/mL of bovine pituitary extract and 5 ng/mL of recombinant rat epidermal growth factor. Cells were placed into the culture flasks of 25 cm^2 and incubated at 37°C in a humidified atmosphere of 5% CO_2.

Immunofluorescence

For immunofluorescence, keratinocytes were plated on 6 mm round glass cover slides and cultured in 24-well plates for 24 hours before fixation with 4% *p*-formaldehyde. Cells were permeabilized with Triton X-100 (0.5%) and blocked with 3% bovine serum albumin (Thermo Fisher Scientific) for 1 hour. The slides were first incubated with the rabbit anti-ClC-2 primary antibody (1:50, Abcam, Cambridge, UK) overnight at 4°C and then with the fluorophore-conjugated secondary antibody (Abcam). After washing with PBS, the slides were labeled by DAPI (5 mg/mL, Beyotime Institute of Biotechnology, Haimen, People's Republic of China) at room temperature. Finally, the slides with cells were inverted onto glass slides, sealed with nail varnish, and examined under a confocal microscope (C1Si, Nikon, Tokyo, Japan). The focus was adjusted until the peak signal was obtained, and then the images were acquired.

Isolation of total RNA and real-time polymerase chain reaction (RT-PCR)

Total RNA was extracted from keratinocytes using Trizol (Thermo Fisher Scientific, Waltham, MA, USA) and treated with DNase (Qiagen NV, Venlo, the Netherlands) according to manufacturer's protocol. RNA was then extracted with phenol/chloroform/isoamylalcohol, precipitated, and then resuspended in 1 mM sodium citrate of pH 6.4. Oligonucleotide primers for ClC-2 amplification were designed using Primers Express software (PE Applied Biosystems). The following are sequences for ClC-2 forward primer, 5′-GGAGCGGACTTCTTTGCAC-3′; ClC-2 reverse primer 5′-TGCTGGTGACATAAG CATGG-3′; GAPDH forward primer, 5′-ACAGCAACAGGGTGG TGGAC-3′; and GAPDH reverse primer, 5′-TTTGAGGGTGCAGCGAACTT-3′. RT-PCR was performed in a RT-PCR detection system (Takara Biotechnology, Ohtsu, Japan). The cycling conditions were as follows: 95°C for 15 seconds, 40 cycles of 95°C for 15 seconds, and 60°C for 30 seconds. The relative levels of ClC-2 mRNA transcripts were normalized to the control GAPDH. Data were analyzed using the $2^{-\Delta\Delta Ct}$ method.

Western blot analysis

Keratinocytes were washed with PBS once and lysed with the lysis buffer (KeyGEN BioTECH, Nanjing, People's Republic of China). The total protein was quantified with Coomassie Brilliant Blue. The equal amounts of protein

samples were separated by SDS-PAGE and transferred to PVDF membranes (Bio-Rad Laboratories Inc., Hercules, CA, USA), which were then blocked at room temperature for 1 hour in blocking solution. The membranes were incubated with the rabbit monoclonal antibody against ClC-2 (1:500, Abcam), PI3K, p-PI3K (1:200, Cell Signaling Technology, Boston, MA, USA) overnight at 4°C,[17] and then with peroxidase-conjugated goat anti-rabbit secondary antibody (1:1,000) for 1 hour at room temperature. Final detection was accomplished with Luminol reagent (SC-2048; Santa Cruz Biotechnology Inc., Dallas, TX, USA) as described by the manufacturer. The density of bands was analyzed using a Bio-Rad Molecular Imager system.

Scratch wound assay

Keratinocytes (5×10^5 cells per well) were plated into six-well plates in culture medium in triplicate. Twenty-four hours after seeding, culture medium was replaced with a fresh medium supplemented with 4 μg/mL mitomycin (Abcam). After 2 hours of incubation, the confluent cell layers were scratched in line using a sterile pipette tip of 200 μL and washed three times with PBS. Thereafter, fresh culture medium was transferred for another 12 hours. The scratched area was then imaged at magnifications of ×10, and the cell-free space was determined using Image J software (NIH, Rockville, MD, USA). The migratory distance is used to measure the migratory ability of keratinocytes.

Transwell cell migration assay

The chemomigration assay was performed using Transwell (pore size, 8 μm; Costar, NY, USA). The chambers were inserted into a 24-well plate. Cells of 1×10^5 suspended with 200 μL K-SFM were added to the upper chamber. Our preliminary experiment proved that the concentration of SDF-1 at 500 ng/mL is the optimal dose to observe the transwell cell migration (data not shown). Therefore, the chemoattractant SDF-1 (500 ng/mL, Abcam) in K-SFM was added into the lower chamber of each well, and the cells were incubated for 12 hours. The medium and nonmigrated cells in the upper chamber were removed gently by cotton swab. Whereas, the migrated cells in the lower side of the membranes were fixed with *p*-formaldehyde (4%) and stained with crystal violet. Pictures were taken at magnifications of ×10. Cells in six different fields were counted.

Transduction of recombinant lentivirus vectors

HIV-1-based lentivirus vector plasmids that express fusion protein of enhanced green fluorescent protein reporter gene were gifts from Dr Jin Zhang (Department of Immunology, Third Military Medical University, People's Republic of China). CLCN2-shRNA was introduced into pGreenPuro-RNAi vector. Three vectors were designed: Lv-CLCN2-sh1, LvCLCN2-sh2, and Lv-CLCN2-sh3. The pGreenPuro vector, which produces an enhanced green fluorescent protein only, was used as the negative control (Lv-CLCN2-shNC) throughout the study. The packaging plasmid psPAX2 (4.5 μg), the envelope plasmid pMD2G (1.5 μg), and the shRNA-LVs (6 μg) were cotransfected into 293T-cells with 2 M $CaCl_2$ (46.5 μL). At the fourth day postinfection, the culture media containing recombinant lentivirus were centrifuged, filtrated, and stored at −70°C for further studies. For lentiviral transduction, keratinocytes were incubated with lentivirus for 48 hours. The suppression of mRNA expression was analyzed by RT-PCR, and CLC-2 protein levels were detected by Western blotting. The most efficient recombinant vector was used in later experiments.

Electrophysiological studies by whole-cell patch clamp

Patch-clamp pipettes are soaked in solution (70 mM CsCl, 1 mM $MgCl_2$, 10 mM HEPES, and 2 mM Na_2ATP [pH 7.2]). The hypotonic bath solution (160 mosmol/L) contained 2 mM $CaCl_2$, 10 mM HEPES, 70 mM NaCl, 0.5 mM $MgCl_2$, and 10 mM D-glucose (pH 7.4). The isotonic solution (280 mosmol/L) contained 2 mM $CaCl_2$, 10 mM HEPES, 70 mM NaCl, 0.5 mM $MgCl_2$, and 140 mM D-glucose (pH 7.4). All reagents were purchased from Sigma-Aldrich (St Louis, MO, USA). The osmotic pressure of the pipette and bath solutions was monitored by an osmometer (Osmomat 30, Gonotec, Germany). The detailed methods for whole-cell patch clamp were performed according to the previous studies.[1,7,9]

Statistical analysis

Data for all measurements are expressed as the mean ± SD. SPSS system for Windows version 18.0 (SPSS Inc., Chicago, IL, USA) was used for statistical analysis. Difference between different experimental groups was determined by one-way analysis of variance. Statistical difference between two groups was performed by the Student's *t*-test. $P<0.05$ was considered to be statistically significant.

Results

Inhibition of ClC-2 expression, cell migration, and $I_{Cl,vol}$ in HG

ClC-2 channels immunoreactivity was observed in isolated keratinocytes cultured from the back of newborn rats.

Figure 1A showed immunofluorescence labeling of ClC-2 and suggested that ClC-2 protein localize in the plasma membrane in rat keratinocytes. Also, the ClC-2 in NG, high mannitol (HM), and HG groups is also localized in the plasma membrane in keratinocytes (data not shown).

To assess the effects of HG on keratinocytes, we cultured rat keratinocytes in HG (25 mM, supplemented to K-SFM), using NG (6 mM) or HM (25 mM) as controls. For the selection of the glucose concentration, we have also tried the other concentration of glucose treatment; however, we found that the concentration of 25 mM is the minimum dose required to inhibit the cell migration (data not shown).

After 7 days of culture,[19] keratinocytes were subjected to different experimental treatments. RT-PCR was performed to measure expression of CLC-2 on mRNA level, and the relevant protein levels were detected by Western blot in keratinocytes of NG, HM, and HG groups after 1 week of culture, respectively. As shown in Figure 1, keratinocytes in HG group showed a lower level of protein expression (Figure 1B and C) and mRNA (Figure 1D) compared to the NG group ($P<0.01$). No significant difference was observed between the NG and HM groups ($P>0.05$).

To investigate the effects of HG on keratinocyte migration, in vitro scratch wound assay and transwell cell migration assay were used. The results of the scratch wound assay demonstrated that the migratory distance of keratinocytes in NG group was significantly higher compared with that in HG concentration ($P<0.01$, Figure 2A and C). To confirm the results of scratch wound assay, transwell assay was used. As shown in Figure 2B and C, the results showed that the number of keratinocytes migrated through pore in

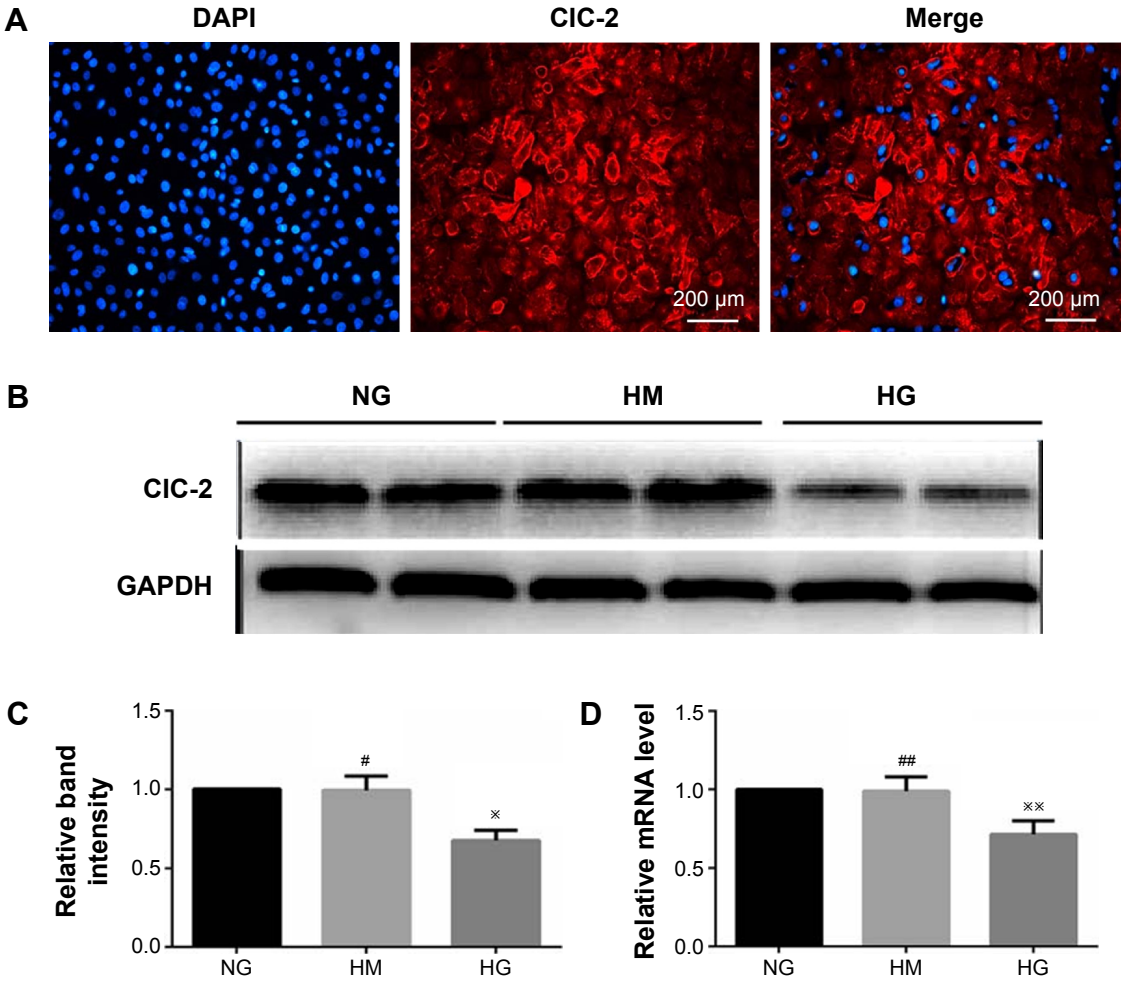

Figure 1 Expression of CIC-2 in keratinocytes exposed to different culture medium.

Notes: (**A**) Immunofluoresence of CIC-2 channels expressed in rat keratinocytes. (**B–D**) High concentration of glucose inhibits expression of CLC-2 on mRNA and protein levels. Keratinocytes were pretreated with normal glucose (6 mM), high mannitol (25 mM), or high glucose (25 mM) concentration medium for 7 days. Real-time PCR and Western blotting was performed and data represented as mean ± SD of triplicate experiments. $^{\#}P$, $^{\#\#}P>0.05$ vs NG or control, $^{※}P<0.05$ vs NG or control, $^{※※}P<0.01$ vs NG or control.

Abbreviations: PCR, polymerase chain reaction; SD, standard deviation; NG, normal glucose; HM, high mannitol; HG, high glucose.

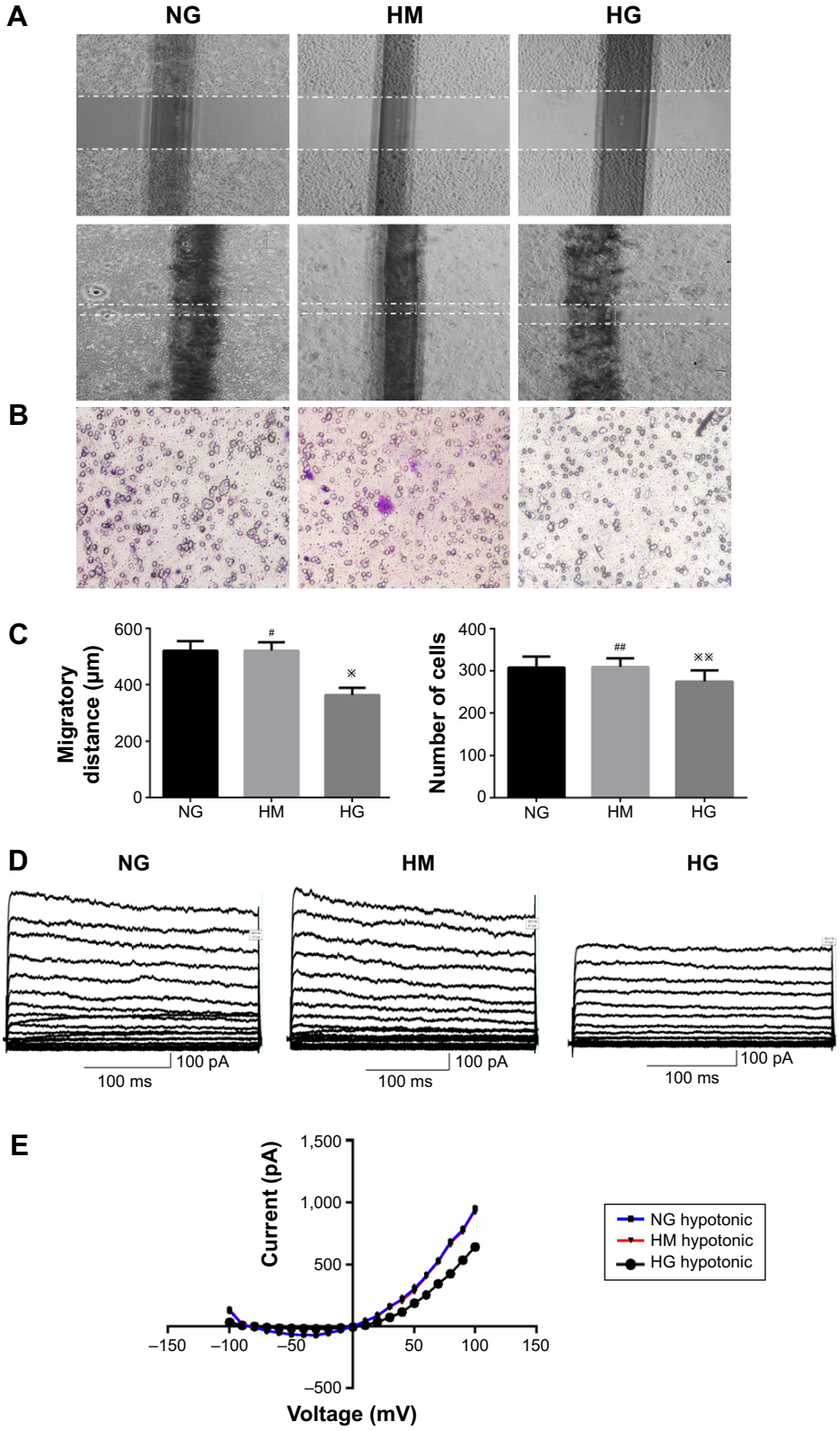

Figure 2 High glucose downregulated the migratory capacity of keratinocytes and volume-activated Cl^- currents.

Notes: Keratinocyte migration was assessed by in vitro scratch wound assay (**A**) and transwell cell migration assay (**B**). The migratory ability of keratinocytes was determined by migratory distance and keratinocytes cells in lower layer (**C**). (**D**) Volume-activated Cl^- was recorded in different conditions. Cells were held at –70 mV and stepped from –100 mV to +100 mV for 300 ms with a 1-second interval repeatedly. Current was recorded under 47% hypotonic bath solution to activate a large current. (**E**) The current–voltage relationships under isotonic and hypotonic condition. The data shown here (mean ± SD) are from one representative experiment performed six times with similar results. $^{\#}P$, $^{\#\#}P>0.05$ vs NG or control, $^{※}P<0.05$, and $^{※※}P<0.01$ vs NG or control.

Abbreviations: NG, normal glucose; HM, high mannitol; HG, high glucose.

HG group was smaller than that in NG group ($P<0.01$), indicating that the HG plays an inhibitory role in keratinocyte migration.

To further investigate the role of HG in keratinocyte migration, the patch-clamp technique was used to assess the alteration of $I_{Cl,vol}$. As shown in Figure 2D, currents were small and stable when the keratinocytes were bathed in isotonic solution. Large currents were activated when the cell was exposed to a 47% hypotonic solution for 1–2 minutes and reached a peak and leveled off in 3–5 minutes. In NG group, similar results were obtained in 11 cells with a mean current of 36.45±4.05 pA under isotonic conditions and 953.22±13.77 pA (peak current) in hypotonic solution at the +100 mV step. These results indicated that the hypotonicity-activated current was sensitive to cell volume alteration. As shown in Figure 2D, the hypotonicity-activated current presented mild outward rectification. There was negligible even no time-dependent inactivation of the current at +100 mV. When the voltage was stepped from −100 mV to +100 mV, the current still showed no obvious time-dependent inactivation (data not shown). The current–voltage relationships under isotonic and hypotonic conditions are shown in Figure 2E. The reversal potential of the hypotonicity-activated current was −8.21±0.74 mV (n=11), which was close to the calculated equilibrium potential for Cl^-. In our experiments, the concentration of Cl^- in pipette solution was almost equal to that in bath solution. These suggest that the main component of the current was $I_{Cl,vol}$. The hypotonicity-activated Cl^- currents recorded from HG keratinocytes were quite different from those from NG cells. In the HG group, the hypotonicity-induced currents were activated more slowly and the peak currents were inhibited. The whole-cell current activated by the hypotonic solution (at the +100 mV step) was reduced from a peak of 953.22±13.77 pA (n=11) in the control cells to 643.86±10.32 pA (n=10; $P<0.01$) in the cells exposed to HG condition. However, there was no significant difference between the peak currents of HG group and HM group (data not shown).

Effect of ClC-2 shRNA on ClC-2 expression in keratinocytes

We used a lentiviral vector system to inhibit the expression of ClC-2 to mimic the ClC-2 inhibitory in HG. Keratinocytes were transfected with either Lv-CLCN2-sh vectors or Lv-CLCN2-shNC vectors, and the ClC-2 mRNA and protein levels were determined by RT-PCR and Western blot. As shown in Figure S1, the mRNA levels of ClC-2 were downregulated in all three designed shRNA inhibitory keratinocytes. However, the ClC-2 silencing induced by Lv-CLCN2-sh1 was greater than that of the others. In addition, Western blotting demonstrated that the Lv-CLCN2-sh1 keratinocytes generated the least ClC-2 protein expression. Therefore, we concluded that Lv-CLCN2-sh1 transfection was functional for silencing expression of ClC-2.

Downregulation of ClC-2 by shRNA inhibits cell migration and $I_{Cl,vol}$ of keratinocytes

Figure 3A showed representative images of keratinocytes migratory abilities. The migratory distance of Lv-CLCN2-sh group was decreased compared with the normal control (NC) and Lv-CLCN2-shNC groups (Figure 3C). Consistently, similar result was obtained in transwell assay, and the migrated cells in lower layer in shRNA group were less than control groups (Figure 3B and C).

Furthermore, we investigated the relationship between ClC-2 and $I_{Cl,vol}$. As described previously, cells were bathed in isotonic perfusate and 160 mosmol to induce $I_{Cl,vol}$. Whole-cell currents under both isotonic and hypotonic conditions were recorded from keratinocytes of NC, Lv-CLCN2-shNC, and Lv-CLCN2-sh groups. In the Lv-CLCN2-sh group, the whole-cell peak current (at the 100 mV) was reduced to 480.89±31.57 pA (n=9, $P<0.01$, Figure 3D). Keratinocytes transfected with Lv-CLCN2-shNC did not affect the hypotonic-activated current (Figure 3D; n=11, $P>0.05$). The current–voltage relationships under isotonic and hypotonic conditions are shown in Figure 3E.

Effects of PI3K inhibitor on ClC-2 expression, cell migration, and $I_{Cl,vol}$ of normal keratinocytes

To determine the endogenous mechanism of alteration of CLC-2 in HG condition, Western blotting was performed to ascertain whether p85 subunit of PI3K undergoes tyrosine phosphorylation using monoclonal antibody against p-PI3K. We found that total PI3K was not significantly altered in keratinocytes cultured in HG medium compared with NG medium. There was a significant reduction in the levels of phosphorylated PI3K in cells cultured in HG medium compared with NG medium (Figure 4A and B).

To further analyze the critical role of PI3K in ClC-2 expression and biological function, the specific inhibitor wortmannin (100 nM) were used. We tested keratinocyte migratory abilities and electrophysiology to determine whether the defects of CLC-2 expression and cell migration seen in HG keratinocytes could be reproduced. Keratinocytes were grown

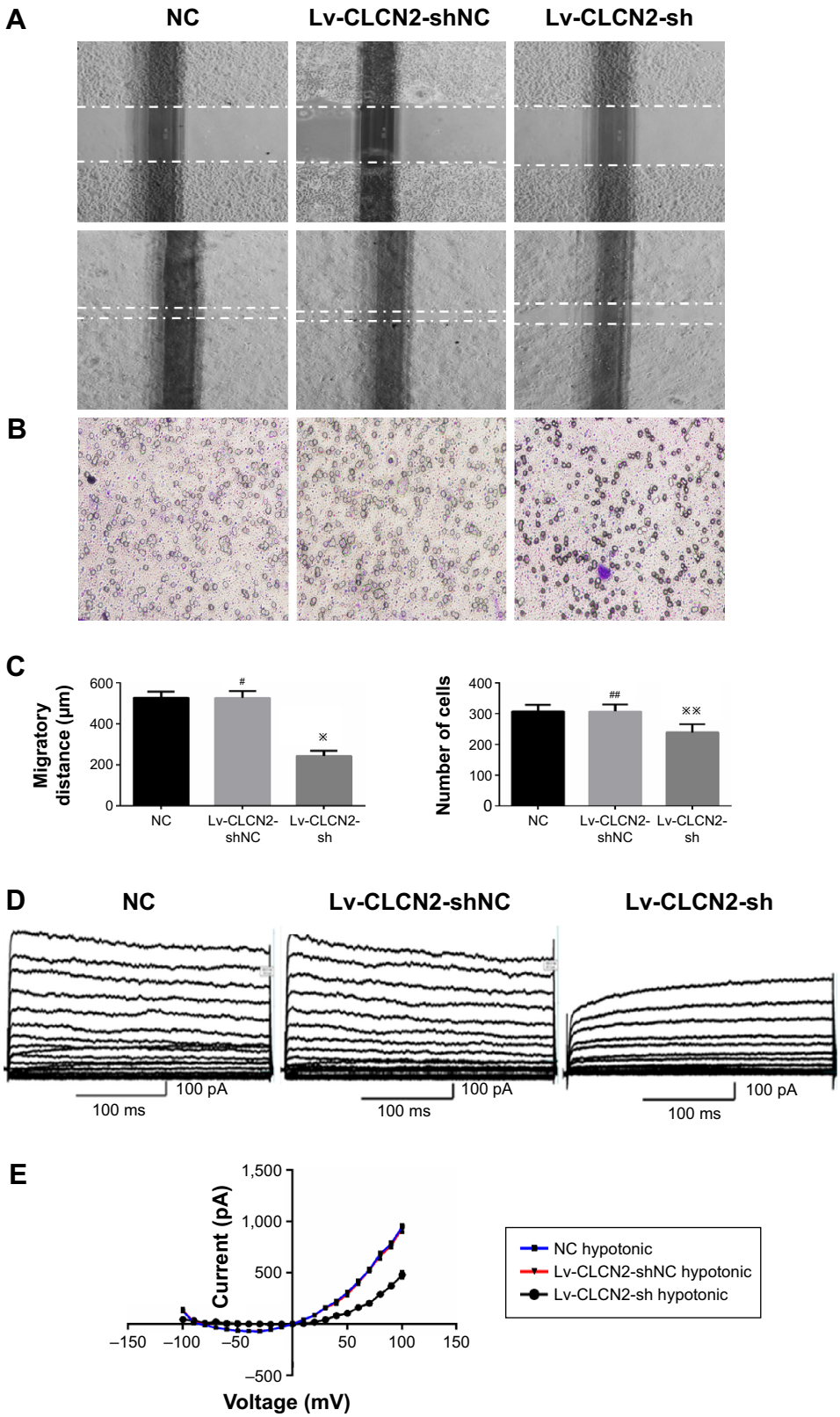

Figure 3 Lv-CLCN2-sh vector downregulated the migratory capacity of keratinocytes and volume-activated Cl^- currents.

Notes: Keratinocyte migration was assessed by in vitro scratch wound assay (**A**) and transwell cell migration assay (**B**). The migratory ability of keratinocytes was determined by migratory distance and keratinocytes cells in lower layer (**C**). (**D**) Volume-activated Cl^- was recorded in different conditions. Cells were held at –70 mV and stepped from –100 mV to +100 mV for 300 ms with a 1-second interval repeatedly. Current was recorded under 47% hypotonic bath solution to activate a large current. (**E**) The current–voltage relationships under isotonic and hypotonic condition. The data shown here (mean ± SD) are from one representative experiment performed six times with similar results. $^{\#}P$, $^{\#\#}P>0.05$ vs Lv-CLCN2-shNC or NC, $^{※}P<0.05$, and $^{※※}P<0.01$ vs Lv-CLCN2-shNC or NC.

Abbreviations: SD, standard deviation; NC, normal control.

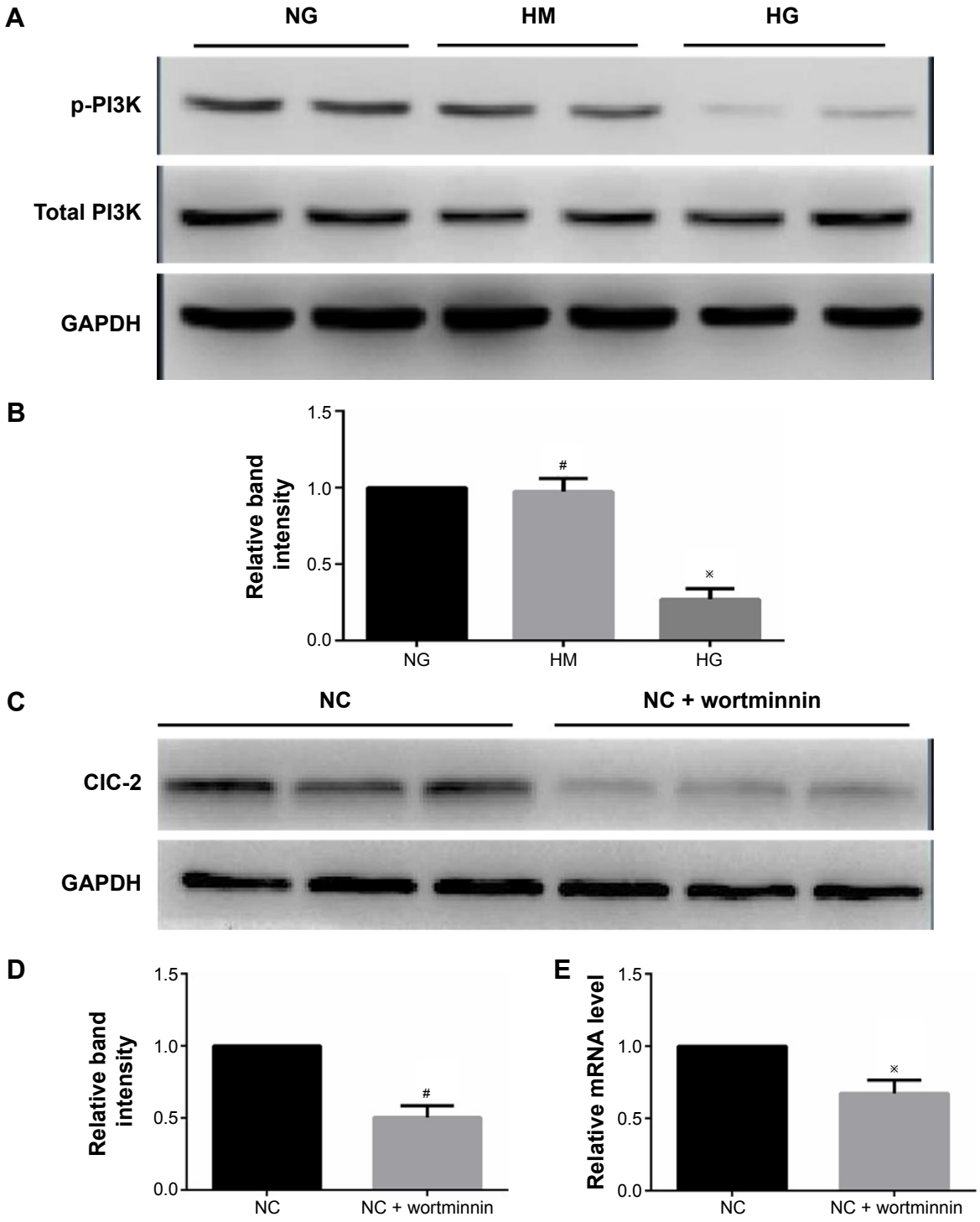

Figure 4 PI3K is involved in the decline of ClC-2 in keratinocytes exposed to high glucose.
Notes: (**A**, **B**) Expression of PI3K and p-PI3K in keratinocytes treated with different medium. Keratinocytes were cultured in normal glucose, high mannitol, and high glucose conditions for 7 days and lysated with SDS lysis buffer, respectively. (**C**–**E**) Expression of ClC-2 in keratinocytes treated with wortminnin. Keratinocytes were treated with 100 nM wortminnin and lysated with SDS lysis buffer. The expression of ClC-2 was detected by Western blotting and RT-PCR. $^{\#}P>0.05$ vs NC, $^{※}P<0.01$ vs NC.
Abbreviations: RT-PCR, real-time polymerase chain reaction; NG, normal glucose; HM, high mannitol; HG, high glucose; NC, normal control.

in NG concentrations and pretreated with 100 nM wortmannin 2 hours before the following procedures. RT-PCR and Western blotting revealed that ClC-2 mRNA expression and ClC-2 protein level in wortmannin-treated keratinocytes were significantly downregulated (Figure 4C–E).

Both scratch wound and transwell cell migration assays also indicated that wortminnin could significantly inhibit migration of keratinocytes (Figure 5A–C). We also found that, after treatment with wortminnin, the electrophysiological difference was significant with attenuated peak currents of

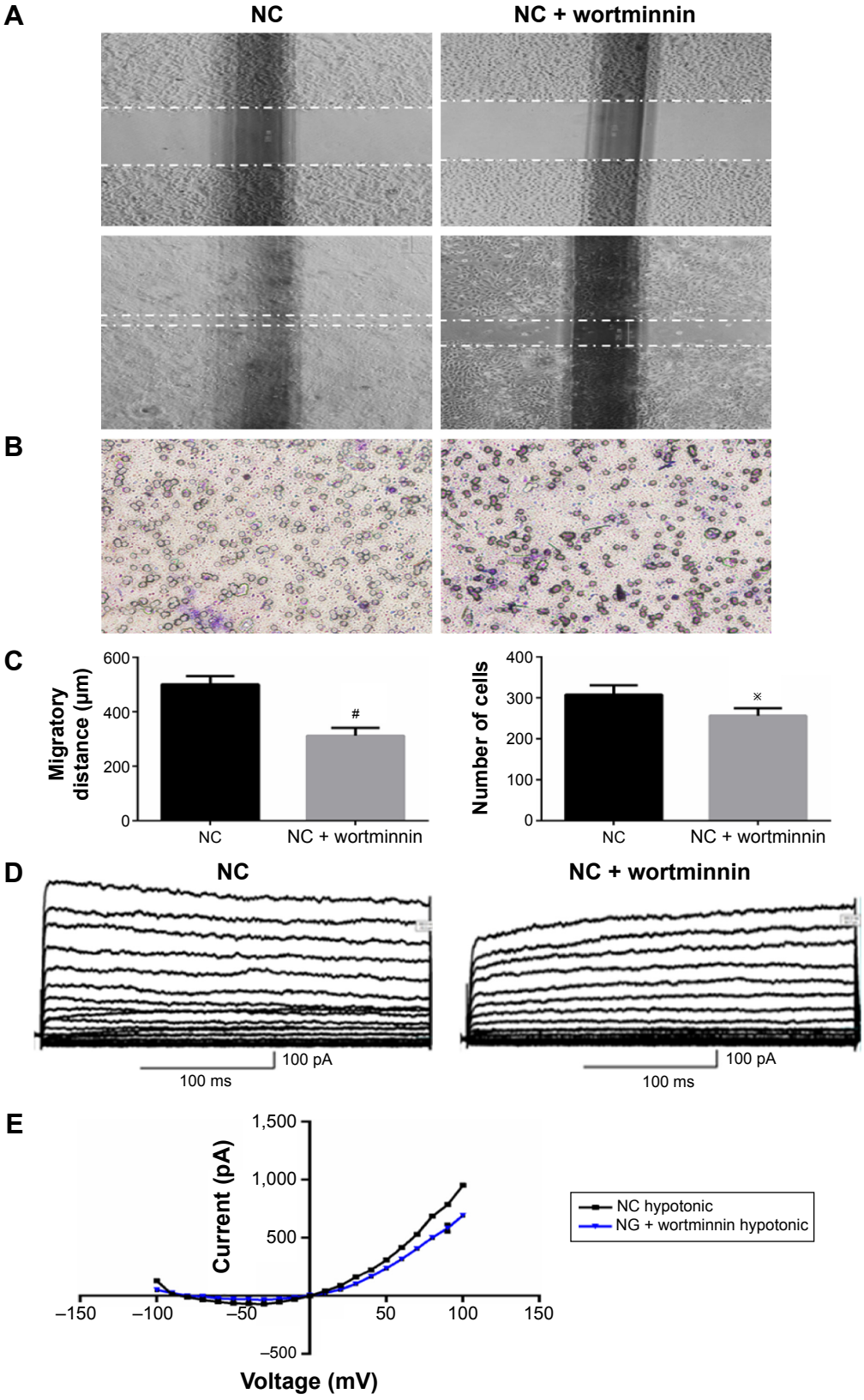

Figure 5 PI3K pathway inhibitor wortminnin downregulated the migratory capacity of keratinocytes and volume-activated Cl^- currents.

Notes: Keratinocyte migration was assessed by in vitro scratch wound assay (**A**) and transwell cell migration assay (**B**). The migratory ability of keratinocytes was determined by migratory distance and keratinocytes cells in lower layer (**C**). (**D**) Volume-activated Cl^- was recorded in different conditions. Cells were held at –70 mV and stepped from –100 mV to +100 mV for 300 ms with a 1-second interval repeatedly. Whole-cell currents recorded in different voltage in normal cells and wortminnin-treated cells, respectively. Current was recorded under 47% hypotonic bath solution to activate a large current. (**E**) The current–voltage relationships under isotonic and hypotonic condition. The data shown here (mean ± SD) are from one representative experiment performed six times with similar results. $^{\#}P>0.01$ vs NC, $^{※}P<0.05$ vs NC.

Abbreviations: SD, standard deviation; NC, normal control; NG, normal glucose.

694.24±24.59 pA (at the 100 mV; n=9, $P<0.01$), as depicted in Figure 5D and E.

Discussion

The skin serves as protective barrier for the underneath organs against the outside world. The deficiency of the cutaneous integrity must be rapidly and efficiently mended via wound healing process. Generally, this process consists of a series of events, including re-epithelialization, remodeling of matrix, and angiogenesis.[20,21] One of these events, re-epithelialization, which requires keratinocyte migration and proliferation, is essential to rebuild a barrier after wounding.[7] Accumulating evidences have indicated that hyperglycemic conditions contribute to impair the migratory potential of keratinocytes and thus lead to delayed wound healing in DM patients.[22,23] In the present study, we show that exposure of keratinocytes to a HG (25 mM) concentration significantly inhibited the ClC-2 expression, $I_{Cl,vol}$, migration potential and phosphorylated PI3K as compared to the control group. Lentivirus-mediated RNAi knockdown of ClC-2, which is designed to mimic the ClC-2 inhibitory condition in HG concentration, significantly inhibited $I_{Cl,vol}$ and migratory abilities of keratinocytes. We further found that the inhibition of the PI3K signaling pathway by wortmannin could downregulate the ClC-2 protein levels and sequentially impede the migratory potential of rat keratinocytes.

HG concentration (25 mM) in cell culture medium has been used to mimic hyperglycemic internal environment of DM patient. Hyperglycemic conditions have been previously demonstrated to decrease cultured keratinocyte mobility.[24,25] In the present study, we further confirm that migratory abilities of rat keratinocytes exposed to HG concentration medium is inhibited compared with NG medium after 7 days of cultivation.

Many experiments have been proposed to interpret the procedure of cell migration, such as amoeboid movement. Briefly, after activation, cells are polarized and move along a front-to-back axis, and a flat and mobile characteristic lamellipodium is formed at the leading edge, which pulls the cell forward via actin polymerization.[26] Contraction of myosin II in the posterior of migrating cells propels the cell forward.[27] However, neglecting of the complicated molecular mechanism, the procedures mentioned earlier is always accompanied by the alteration of local cell volume. Ion channels are membrane proteins controlling ion fluxes across plasma membranes and able to efficiently regulate global cell volume. By creating local osmotic gradients, ion channels facilitate the swelling or shrinking of cellular processes.[28] VACC has been proposed to account for the alteration of migratory abilities in tumor cells.[29,30] The almost ubiquitous ClC-2, one of the nine ClC family that activated by membrane hyperpolarization, a low extracellular pH, and osmotic cell swelling,[31] is considered to help regulate the volume-activated chloride current.[32] In this study, we speculate that ClC-2 plays a critical role in the migratory ability of keratinocytes. RT-PCR and Western blot assay demonstrate that HG keratinocytes have a lower expression level of ClC-2 mRNA and protein than normal keratinocytes, and this is the only study to our knowledge. In addition, we found that $I_{Cl,vol}$ was inhibited in HG keratinocytes corresponding to the inhibition of keratinocyte migration. These results suggest that ClC-2 may be involved in impeding keratinocyte migration in HG condition.

By confirming the role of ClC-2 in keratinocyte migration, lentivirus vectors were introduced in our study. We designed an experiment to investigate the suppression of keratinocyte by targeting the expression of ClC-2 to mimic the ClC-2 inhibitory condition in HG concentration. Numerous vectors have been utilized to infect different cells and to express shRNAs in many studies. Among these vectors, lentivirus-based vectors could transfect a large number of genetic messages to target cells efficiently, and furthermore, lentiviruses are able to infect both dividing and nondividing cells with long-term regulation of gene expression.[33,34] Lentiviral-mediated RNAi has been widely used to knock down gene expression in mammalian cells and thus a useful tool for studying gene functions and therapeutic potential for various diseases.[35] These advantages made lentiviral-based vectors the best to study the effect of ClC-2 silencing on keratinocytes. We successfully constructed the pGreenPuro-RNAi lentivirus vector, which could efficiently knock down the expression of ClC-2 mRNA. Significantly, consistent with our hypothesis, migration assay demonstrated that suppression of ClC-2 can result in impeding cell migration. Electrophysiological discoveries also demonstrated an inhibition of $I_{Cl,vol}$.

PI3K is one of the primary downstream intracellular pathways of signaling. Previous studies indicate that the activation of ClC-2 requires the activation of PKC and PI3K, and PI3K inhibitor can suppress IGF-IR-induced ClC-2 upregulation. PI3K also play an important role in cell migration of different cell types.[36] Li et al[37] found that high D-glucose altered PI3K and Akt signaling and leaded to endothelial cell migration dysfunction. Similarly, suppression of the PI3K–Akt pathway was found involved in the decreased adhesion and migration of bone marrow-derived mesenchymal stem cells

from nonobese diabetic mice. Our data also showed that HG concentration impaired the phosphorylation of PI3K, which resulted in inhibition of ClC-2 expression, keratinocytes migration, and $I_{Cl,vol}$.

However, in either siRNA silencing or wortminnin inhibiting cells, the volume-activated chloride currents were not inhibited thoroughly. These indicated that ClC-2 played a partial role rather than a dominant role in volume-activated chloride currents. The critical role of ClC-2 in the cell migration is still unclear. So far, the majority of studies focusing on the connection of VACCs and cell migration or invasion were performed in malignant cells.[30] Whole-cell patch clamp of fetal human nasopharyngeal epithelial cells exhibits volume-activated chloride currents. Chloride channel inhibitor ATP, tamoxifen, and 5-nitro-2-(3-phenylpropylamino) benzoic acid dramatically inhibited the hypotonicity-activated current.[38] Similar results were obtained in human glioma cells, endometrial cancer cells, and Hela cells, and the application of chloride channel inhibitor reduced chemotactic migration in a dose-dependent manner.[30] One of the molecular candidates for the VACC is probably ClC-2, although there are still some controversies. In glioma cell, ClC-2 and ClC-3 were found located to lamellipodia on the leading edges, placing them in prime location to flux Cl^- and facilitate migration. As chloride channels play an important role in cell migration, there must be some channels that work in concert to allow the efflux of cations to maintain electroneutrality. Cancer cells expressed several types of K^+ channels contributing to migration such as calcium-activated potassium channels (BK), which leaded to a 60%–80% inhibition of glioma cell migration when treated with pharmacological inhibitors. shRNA knockdown can reduce the expression of BK channels and eliminates iberiotoxin-sensitive currents by 70%.[39] It is believed that K^+ and Cl^- enter the leading edge of lamellipodia, leading to local cell swelling obligatory for cell migration. An increase in cell volume initiated the RVD process to get its normal volume through the activation of ion channel, such as K^+ channels, Cl^- channels, and other types of channels and transporters. The activation of $I_{Cl,vol}$ is of importance for RVD.[11] Although many of the mechanisms of cell migration are shared or identical, it is quite necessary to ascertain the individual mechanisms of keratinocyte migration concerning to ClC-2 because of the heterogeneity in cell types. We have not investigated the effect of these chloride channel inhibitors on keratinocyte migration. What is more, whether overexpression or activation of ClC-2 in keratinocytes cultured in HG concentration would accelerate cell migration is waiting to be revealed.

Although our study provided some important data for the therapy with HG for the ClC-2 chloride channels and attenuated cell migration of rat keratinocytes, there were also some limitations that should be improved in the future studies. For instance, the gain of function experiments of the ClC-2 in keratinocytes were omitted, and the in vivo data were not included. Therefore, in the future study, we would investigate the function of ClC-2 in keratinocytes and perform the experiments in the level of in vivo.

In summary, HG concentration inhibited keratinocyte migration through downregulation of ClC-2. ClC-2 expression was downregulated by impairment of PI3K phosphorylation. Although it is still unclear how the ClC-2 channels involve in keratinocyte migration, our findings suggest that ClC-2 channels are the important modulators of cell migration in keratinocytes and may play a role in delayed wound healing processes. We suggest that upregulation of ClC-2 within the keratinocyte should be considered as a target for future therapeutic modalities in protecting the DM patient from chronic delayed wound healing.

Acknowledgments

This work was financially supported by a grant from the National Natural Science Foundation of China (No 81272121).

Author contributions

All authors contributed toward data analysis, drafting and revising the paper and agree to be accountable for all aspects of the work.

Disclosure

The authors report no conflicts of interest in this work.

References

1. Cakirca M, Karatoprak C, Zorlu M, et al. Effect of vildagliptin add-on treatment to metformin on plasma asymmetric dimethylarginine in type 2 diabetes mellitus patients. *Drug Des Devel Ther*. 2014;8:239–243.
2. Singer AJ, Clark RA. Cutaneous wound healing. *New Eng J Med*. 1999; 341(10):738–746.
3. Falanga V. Wound healing and its impairment in the diabetic foot. *Lancet*. 2005;366(9498):1736–1743.
4. Medina A, Scott PG, Ghahary A, Tredget EE. Pathophysiology of chronic nonhealing wounds. *J Burn Care Rehabil*. 2005;26(4):306–319.
5. Woodley DT, Chen JD, Kim JP, et al. Re-epithelialization. Human keratinocyte locomotion. *Dermatol Clin*. 1993;11(4):641–646.
6. Santoro MM, Gaudino G. Cellular and molecular facets of keratinocyte reepithelization during wound healing. *Exp Cell Res*. 2005;304(1): 274–286.
7. Usui ML, Mansbridge JN, Carter WG, Fujita M, Olerud JE. Keratinocyte migration, proliferation, and differentiation in chronic ulcers from patients with diabetes and normal wounds. *J Histochem Cytochem*. 2008; 56(7):687–696.

8. Bullock AJ, Barker AT, Coulton L, Macneil S. The effect of induced biphasic pulsed currents on re-epithelialization of a novel wound healing model. *Bioelectromagnetics*. 2007;28(1):31–41.
9. Sivamani RK, Garcia MS, Isseroff RR. Wound re-epithelialization: modulating keratinocyte migration in wound healing. *Front Biosci*. 2007; 12:2849–2868.
10. Korogod SM, Kulagina IB. Dynamical electrical states of heterogeneous populations of ion channels in the membranes of excitable cells. *Fiziol Zh*. 2012;58(3):50–59.
11. Sardini A, Amey JS, Weylandt KH, Nobles M, Valverde MA, Higgins CF. Cell volume regulation and swelling-activated chloride channels. *Biochim Biophys Acta*. 2003;1618(2):153–162.
12. Lang F, Busch GL, Ritter M, et al. Functional significance of cell volume regulatory mechanisms. *Physiol Rev*. 1998;78(1):247–306.
13. Sontheimer H. An unexpected role for ion channels in brain tumor metastasis. *Exp Biol Med*. 2008;233(7):779–791.
14. Xu B, Mao J, Wang L, et al. ClC-3 chloride channels are essential for cell proliferation and cell cycle progression in nasopharyngeal carcinoma cells. *Acta Biochim Biophys Sin (Shanghai)*. 2010;42(6):370–380.
15. Zhu L, Yang H, Zuo W, et al. Differential expression and roles of volume-activated chloride channels in control of growth of normal and cancerous nasopharyngeal epithelial cells. *Biochem Pharmacol*. 2012;83(3):324–334.
16. Roman RM, Smith RL, Feranchak AP, Clayton GH, Doctor RB, Fitz JG. ClC-2 chloride channels contribute to HTC cell volume homeostasis. *Am J Physiol Gastrointest Liver Physiol*. 2001;280(3):G344–G353.
17. Huang ZM, Prasad C, Britton FC, Ye LL, Hatton WJ, Duan D. Functional role of CLC-2 chloride inward rectifier channels in cardiac sinoatrial nodal pacemaker cells. *J Mol Cell Cardiol*. 2009;47(1):121–132.
18. Comes N, Abad E, Morales M, Borras T, Gual A, Gasull X. Identification and functional characterization of ClC-2 chloride channels in trabecular meshwork cells. *Exp Eye Res*. 2006;83(4):877–889.
19. Lan CC, Wu CS, Huang SM, et al. High-glucose environment inhibits p38MAPK signaling and reduces human beta-defensin-3 expression [corrected] in keratinocytes. *Mol Med*. 2011;17(7–8):771–779.
20. Cheret J, Lebonvallet N, Buhe V, Carre JL, Misery L, Le Gall-Ianotto C. Influence of sensory neuropeptides on human cutaneous wound healing process. *J Dermatol Sci*. 2014;74(3):193–203.
21. Kirsner RS, Eaglstein WH. The wound healing process. *Dermatol Clin*. 1993;11(4):629–640.
22. Blakytny R, Jude E. The molecular biology of chronic wounds and delayed healing in diabetes. *Diabet Med*. 2006;23(6):594–608.
23. Shan GQ, Zhang YN, Ma J, et al. Evaluation of the effects of homologous platelet gel on healing lower extremity wounds in patients with diabetes. *Int J Low Extrem Wounds*. 2013;12(1):22–29.
24. Marston WA; Dermagraft Diabetic Foot Ulcer Study Group. Dermagraft Diabetic Foot Ulcer Study G: risk factors associated with healing chronic diabetic foot ulcers: the importance of hyperglycemia. *Ostomy Wound Manage*. 2006;52(3):26–28, 30, 32 passim.
25. Lan CC, Liu IH, Fang AH, Wen CH, Wu CS. Hyperglycaemic conditions decrease cultured keratinocyte mobility: implications for impaired wound healing in patients with diabetes. *Br J Dermatol*. 2008;159(5):1103–1115.
26. Nabi IR. The polarization of the motile cell. *J Cell Sci*. 1999;112(pt 12): 1803–1811.
27. Conrad PA, Giuliano KA, Fisher G, Collins K, Matsudaira PT, Taylor DL. Relative distribution of actin, myosin I, and myosin II during the wound healing response of fibroblasts. *J Cell Biol*. 1993; 120(6):1381–1391.
28. Schwab A, Nechyporuk-Zloy V, Fabian A, Stock C. Cells move when ions and water flow. *Pflugers Arch*. 2007;453(4):421–432.
29. Cuddapah VA, Sontheimer H. Molecular interaction and functional regulation of ClC-3 by Ca2+/calmodulin-dependent protein kinase II (CaMKII) in human malignant glioma. *J Biol Chem*. 2010; 285(15):11188–11196.
30. Mao J, Chen L, Xu B, et al. Volume-activated chloride channels contribute to cell-cycle-dependent regulation of HeLa cell migration. *Biochem Pharmacol*. 2009;77(2):159–168.
31. Jordt SE, Jentsch TJ. Molecular dissection of gating in the ClC-2 chloride channel. *EMBO J*. 1997;16(7):1582–1592.
32. Grunder S, Thiemann A, Pusch M, Jentsch TJ. Regions involved in the opening of CIC-2 chloride channel by voltage and cell volume. *Nature*. 1992;360(6406):759–762.
33. Yu X, Zheng B, Chai R. Lentivirus-mediated knockdown of eukaryotic translation initiation factor 3 subunit D inhibits proliferation of HCT116 colon cancer cells. *Biosci Rep*. 2014;34(6):e00161.
34. Ying X, Zhang R, Wang H, Teng Y. Lentivirus-mediated RNAi knockdown of LMP2A inhibits the growth of nasopharyngeal carcinoma cell line C666-1 in vitro. *Gene*. 2014;542(1):77–82.
35. Kim DH, Rossi JJ. Strategies for silencing human disease using RNA interference. *Nat Rev Genet*. 2007;8(3):173–184.
36. Seo M, Lee S, Kim JH, et al. RNAi-based functional selection identifies novel cell migration determinants dependent on PI3K and AKT pathways. *Nat Commun*. 2014;5:5217.
37. Li L, Xia Y, Wang Z, et al. Suppression of the PI3K-Akt pathway is involved in the decreased adhesion and migration of bone marrow-derived mesenchymal stem cells from non-obese diabetic mice. *Cell Biol Int*. 2011;35(9):961–966.
38. Sun X, Chen L, Luo H, et al. Volume-activated chloride currents in fetal human nasopharyngeal epithelial cells. *J Membr Biol*. 2012;245(2): 107–115.
39. Weaver AK, Bomben VC, Sontheimer H. Expression and function of calcium-activated potassium channels in human glioma cells. *Glia*. 2006;54(3):223–233.
40. Francis R, Xu X, Park H, et al. Connexin43 modulates cell polarity and directional cell migration by regulating microtubule dynamics. *PLoS One*. 2011;6(10):e26379.

Supplementary material

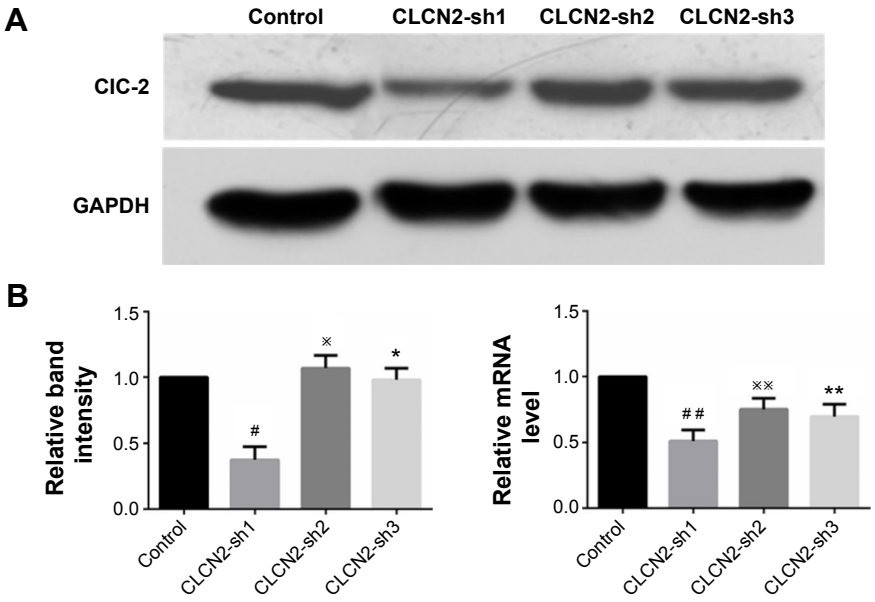

Figure S1 Effect of siRNA against mRNA on ClC-2 protein and mRNA expressions.

Notes: (**A**) The western blot analysis of CLC-2 and GAPDH protein expression. (**B**) Statistical analysis of CLC-2 and GAPDH expression. The CLCN2-sh1 significantly down-regulated the ClC-2 protein level and showed relative expression of ClC-2 mRNA detected by RT-PCR. Values expressed as mean ± SD, calculated from three independent experiments; $^{\#}P$, $^{\#\#}P<0.05$ compared with control, $^{※}P$, $^{※※}P<0.05$ compared with CLCN2-sh2. $^{*}P$, $^{**}P<0.05$ compared with CLCN2-sh3.

Abbreviations: RT-PCR, real-time polymerase chain reaction; SD, standard deviation.